25th IMEKO TC4 International Symposium
23rd International Workshop on ADC and DAC Modelling and Testing
IMEKO TC-4 2022
Brescia, Italy / September 12-14, 2022

Design and validation of a reference multi-sensor cinemometer for law enforcement applications

Seif Ben-Hassine[1], Dominique Renoux[1], Catherine Yardin[1], Jabran Zaouali[1], Jimmy Dubard[1], Jean-Marie Lerat[1], Pierre Betis[1], Isabelle Blanc[1]

[1]*Laboratoire National de métrologie et d'Essais (LNE), France, Seif.Benhassine@lne.fr*

***Abstract* – This paper describes a new reference multi-sensor cinemometer designed for the purpose of the homologation of radars dedicated to road traffic control. It is intended to replace the actual reference cinemometer deployed in France, which is not longer adapted to the new generation of radars as it delivers less measurement parameters and has less detection capabilities. The new multi-sensor cinemometer system is presented by detailing the operation of its processing units. The fusion of measurements provided by the various sensors is explained. The computation of the reference speed and its associated uncertainty is exposed. Finally, on-site measurement results are presented by comparing the system with the actual reference cinemometer.**

I. INTRODUCTION

The rapid evolution of cinemometer technology with the use of multi-target tracking functions, that enables high rate of target detection and curvilinear speed measurement, requires an evolution of the verification techniques and reference cinemometer. Currently, the method used to assess the speed accuracy of traffic cinemometers in France is the comparison to a standard system based on a single Continuous-Wave (CW) radar, called HADER. This one delivers an instantaneous speed measurement whose traceability to the International System of Units (SI) is ensured by the calibration of the emitted RF frequency and of the measured Doppler shift of the echoed RF wave. This reference system, operating at 24 GHz, is equipped with a static parabolic antenna emitting a narrow electromagnetic beam and is used at a 25° angle with the road. This system is limited in application with respect to new devices as it does not allow the speed measurement on curvilinear roads. Furthermore, it is hightly sensitive to masking effects on multiple lane roads.

In this paper, we present a new multi-sensor cinemometer system of increased capacities and facilities while keeping the required level of uncertainty. This system allows to compete with the features of new cinemometer technologies:

- Multi-lane measurement without masking effect.
- Multi-target measurement.
- Configurable infraction zone.
- Curved track measurement.
- Speed gradient measurement in the infraction zone.

Section II presents the device and its main processing units. Section III deals with the data acquisition unit and describes the different sensor subsystems. Section IV describes the data processing unit which combines the measurement results provided by the various sensors and computes the reference speed. The latter is then compared to the device under test (DUT) measurements by taking into account the measurement uncertainty. Section V discusses the reliability of the designed cinemometer system and gives some results based on the comparison with the reference system HADER. Finally, Section VI concludes this development.

II. OVERALL DESCRIPTION

The system is based on a multi-sensor configuration in order to improve the reliability of the system measurements and to reduce the overall uncertainty. The system consists of an acquisition and processing unit controlling four radars and one lidar speed sensors. The different system components are represented on the diagram in Figure 1.

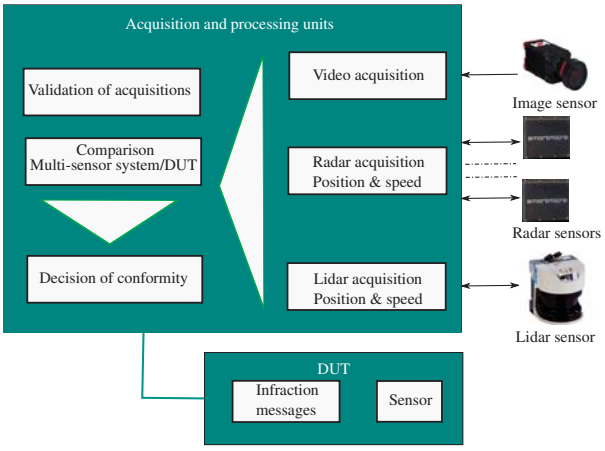

Fig. 1. System block diagram.

The system continuously acquires the speed, time and position information from the lidar and radar

sensors. Concurrently, the alive stream of the camera is timestamped and recorded. The processing unit calculates the reference speed value, its associated uncertainty, and the time for each infraction. The reference time is dispatched by an NTP (Network Time Protocol) server connected to a GPS receiver. The processing unit also enables to extract the associated image at this reference time.

Automatic DUT provides, for each violation a speed value, time and picture that can be compared to those of the developed system. This comparison is made easy by means of a dedicated developed software which displays side by side information of time sorted infractions that can be checked by the pictures display of the vehicle provided both by the system and the DUT.

III. DATA ACQUISITION

A. *Radar subsystem*

The instantaneous speed measurement of the vehicles is carried out by using the Doppler phenomenon in the microwave domain, this is the principle of the radar system [1]. The emitted electromagnetic wave radiates its energy in a privileged direction by means of a directional antenna. After reflection on a moving target, a part of the wave received by the antenna is combined in an electronic mixer circuit with a fraction of the transmitted wave. The Doppler frequency (F_d) obtained from this mixer is proportional to the mobile speed (v) and to the cosine of an angle between the mobile trajectory and the radiation axis of the antenna [2], *i.e.*:

$$F_d = \frac{2v\cos(\alpha)}{\lambda}. \quad (1)$$

with

- v the mobile speed in m/s.
- α the angle between the mobile trajectory and the radiation axis of the antenna in rad.
- λ the emission wavelength in m.

The radars sensors are of type FMCW MIMO (Frequency Modulated Continuous Wave Multiple Input Multiple Output) system. This type offers the target tracking feature. The tracking function of the radar sensor is supported by a B-Spline model to approximate the traffic lane. The parameters used for the configuration of the sensors are the control points of the B-Spline interpolation curve. These control points are calculated from the X-Y coordinates of the points measured at the road middle points [3]. Figure 2 shows a graphical representation of the B-Spline curve associated to the control points. The coordinates of the control points are defined with respect to a reference point located on the mechanical structure of the system.

The radar subsystem is composed of four sensors of type

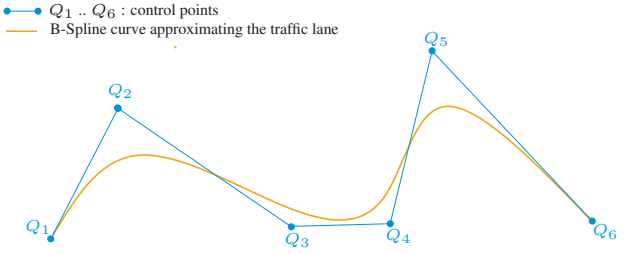

Fig. 2. Graphical representation of B-Spline curve associated to the control Points.

Smartmicro UMRR-11 T132. This type of sensor, with an operating frequency range of 76 GHz to 77 GHz, is designed for multi-lane, multi-object traffic management applications with 4D/HD$^+$ technology [4]. The HD$^+$ resolution means that the sensor allows separating objects according to their speed and their distance from the sensor. The use of a 77 GHz sensor guarantees the absence of interference between a DUT Doppler radar (operating at 24 GHz) and the designed reference cinemometer system. The 77 GHz allows achieving better performances in range, speed accuracy and resolution compared to 24 GHz radar.

Figure 3 presents the electrical architecture of the radar subsystem. The radars perform the position and speed measurements simultaneously on the same target. The use of multi-sensors allows:

- to reduce the cases of masking by positioning the radars at a height between 2,4 m and 2,6 m,
- to increase the redundancy on the detection zone,
- to provide a compromise between the blind zone and the redundancy zone.

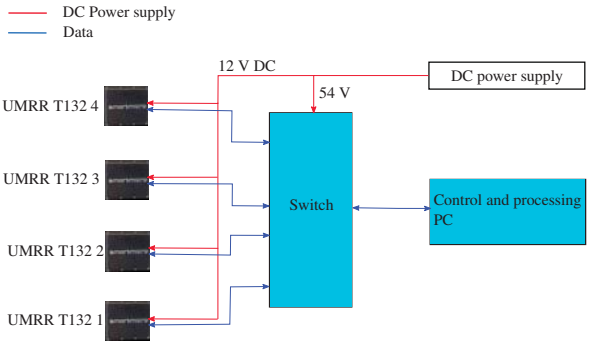

Fig. 3. Electronic architecture of the radar subsystem.

The data are provided by the radar units on an Ethernet UDP bus, with target positions and speed defined with respect to the reference point used for B-Spline definition.

B. *Lidar subsystem*

Lidar (Light detection and ranging) is an opto-electronic measurement device that derives the distance between the

surface of an object and the device (emitter/receiver) from the measurement of the time of flight of a laser pulse. The cinemometer is a 2D lidar based on a rotary pulsed laser emitter/receiver and the velocity can be determined by the difference of distances acquired for several rotations. The rotation frequency is 75 Hz and the angular resolution is 0.5°. The laser emits light at a wavelength of 905 nm.

The lidar cinemometer is integrated by CES Ag from a commercial lidar. It is composed of a 2D lidar unit SICK LMS511-12100, an industrial PC and a customized software for data acquisition and processing.

The data, as a sampled target horizontal profile of the vehicle, recorded by the lidar subsystem for each five rotations and provided by the CESag software are post-processed by a LNE software to provide a set of measured speeds over an interval around the infraction line.

C. *Vision subsystem*

The vision subsystem is composed of a camera, a video recorder from IO industries and a ruggedized PC tablet with IO controlling software. The recorded images are accurately time stamped using transmitted digital NEMA ZDA frames to the tablet and an analog PPS (Pulse Per Second) signal provided to the recorder. These two times information, via serial and analog interface, are provided by the GPS unit. The camera resolution is 4112x2176 and the frame rate is 30 Hz. The optimal exposure time is around 100 μs to avoid kinetic blur. The camera is equipped with a F1/4 20 mm lens. All these features enable to identify the number plate of vehicles under cloudy weather, four lanes highway and high speed up to 300 km/h.

D. *Synchronization of acquisitions*

Lidar and radar acquisitions are time stamped by the clocks of two driving different PCs which are synchronized to the NTP server of the GPS unit, all being connected to the same Ethernet local network. The video recorded stream is also time stamped by two signals, as described in the vision subsystem, provided by the same GPS unit.

Data analysis was performed on trials in order to determine the synchronization of acquisitions. It showed a stable 160 ms time shift between lidar and radars data. The stability of this time shift has been evaluated on acquisitions with short and long durations on several sessions. It is consistent with the specified processing time of the radar sensors and the system design which sets the lidar as a time reference for all acquisitions.

IV. DATA PROCESSING

A. *Data fusion*

The radar and lidar subsystems perform speed measurements independently of each other. These measurements are then combined to improve the reliability of the measurements produced by the system and to decrease the overall uncertainty.

The data are provided in the system reference frame. The fusion process is carried out in steps by considering at each step only two set of sensor's targets. It is firstly applied to the radars. A radar being taken as the initial set of targets, the process consists in associating it with data from a second radar according to a temporal criterion and a spatial criterion applied to each target. This new enlarged set, of fused data for each target, is then compared to the data from the third radar using the same criteria. The process continues until the lidar data are fused. At each step, the unfused targets are kept in the group. The fusion reliability is tested by initializing the process on different sensors.

B. *Computation of the reference speed and its associated uncertainty*

The reference speed value is evaluated in three steps represented in Figure 4.

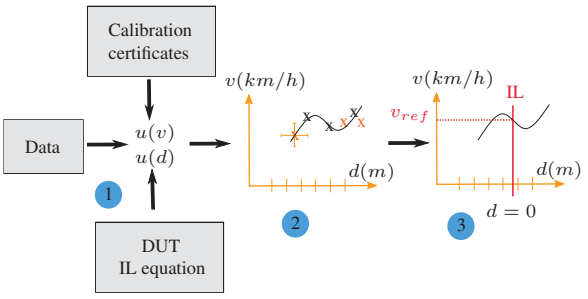

Fig. 4. Computation steps for establishing the reference speed value and the associated uncertainty.

The first step, described before, deals with the input data: the measurement line which is defined according to the infraction line of the DUT, and the fused data issued from the fusion algorithm and their associated uncertainties. These uncertainties have been evaluated separately for each sensor and they take into account the trueness and fidelity components. The radar and lidar uncertainties are decomposed into a constant part and a variable part. These parts correspond to the short and long term uncertainties. In the case of distance measurements d, we have propagated the uncertainties associated to the coordinates x,y returned by the sensors by using the measurement line equation and the measurement model of the distance from the target to the infraction line.

In the second step, a regression model is applied to represent for each target the relationship between the measured speed values v and the distances to the measurement line d. This model is a polynomial of maximum degree 3, quite often degree 0 (constant speed)

or degree 1 (monotonic variation), and its expression is given by:

$$G(d) = b_0 + b_1 d + b_2 d^2 + b_3 d^3. \quad (2)$$

with b_0, b_1, b_2 and b_3 being the model coefficients. They are estimated with GLS (Generalized Least Squares) methods [5] that enables to propagate the uncertainties associated to the data.

In the third step, the model is used to evaluate the reference speed value of the target at the infraction line. This prediction is computed by setting d = 0 and then its expression corresponds to the intercept b_0 of the model whatever the degree of the polynomial:

$$v_{ref} = G(0) = b_0. \quad (3)$$

It follows that the uncertainty associated to the reference speed value is the uncertainty associated to the term b_0.

V. TESTS AND VALIDATION

Different test campaigns were carried out, including lab's simulation tests and tests performed on various real traffic sites, to adjust the system and to assess its performances through comparative and statistical analysis of all collected data. The accuracy of the measured speeds by the system has been assessed using the HADER cinemometer as a reference.

A comparison campaign is performed with the HADER on a two-lane road located in the suburb of Paris. Only the receding lane is used for the test. A photograph of the test setup is presented in Figure 5. The HADER is approximately placed at 7 m from the origin point of the new system, with an orientation angle set at 25° between its main beam and the road axis. This distance and this angle are measured using a tacheometer device. A subsequent correction is then applied on the speed measurements accounting for the measured angle value. Table 1 presents the radar and lidar uncertainties taken as hypotheses for the computation of the reference speed and its associated uncertainty.

Table 1. Radar and Lidar uncertainties used to test the computation algorithm of the reference speed and its associated uncertainty.

	$u(d)$	Constant $u(v)$	Variable $u(v)$
Radar ($v \leq 100$ km/h)	1 m	0.31 km/h	0.36 km/h
Radar ($v > 100$ km/h)	1 m	0.2 %	0.45 %
Lidar	0.04 m	0.2 %	0.22 %

Figure 6 presents the X-Y positions of objects detected by radar 1. We observe that the vehicles trajectories are centered on the B-Spline curve calculated by the radar sensor.

Fig. 5. Measurement campaign on a two-lane road located in the suburb of Paris.

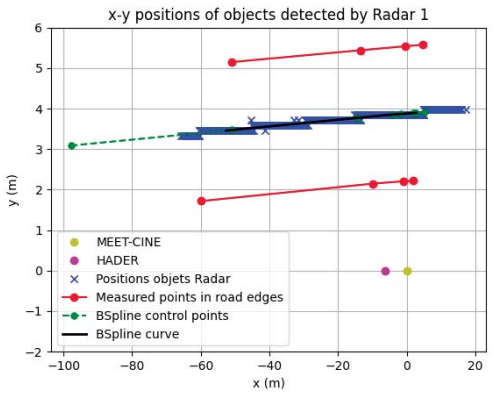

Fig. 6. X-Y positions of objects detected by radar 1.

The data pairing between HADER and the system is performed at the infraction position determined from the actual orientation of HADER antenna and the distance between HADER and the system. The system measurements are interpolated at this position. The time shift between the HADER and the system is evaluated by comparing the timestamps corresponding to the maximum

speeds recorded by both systems. All HADER timestamps are then corrected according to this time shift. The pairing of HADER speed values to the speed values measured by the system is carried out by matching the HADER corrected timestamps with those of the designed system.

The performance of the multi-sensor cinemometer system is evaluated by using the relative difference between HADER speed values and those of each sensor at the intersection coordinate between the HADER radar beam and the road center axis. Table 2 gives a statistical summary of results obtained for several measurement sessions performed the same day with the mean value of the relative difference and its associated standard deviation.

Figures 7 and 8 provide the comparison of the speed values measured by HADER and the sensors (radar 1 and lidar) on the targets detected during the first 10 min measurement session. This comparative study shows a high degree of agreement between the HADER and the multi-sensor cinemometer system. The mean values of differences between each system's sensors and the HADER are all lower than 0.21 %. The associated standard deviations are all lower than 0.57 %. The standard deviations do not vary from one test to another, which reveals that there is no test effect.

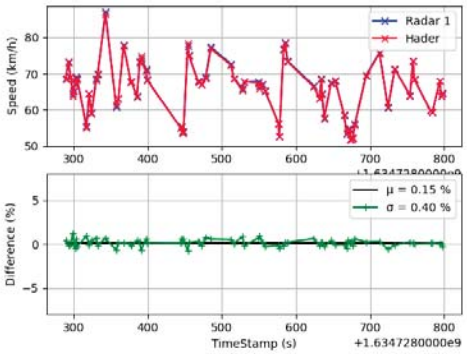

Fig. 7. Pairing results HADER-Radar 1.

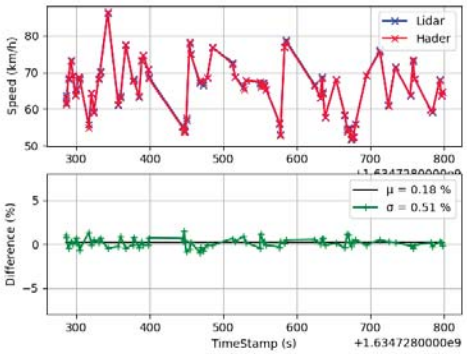

Fig. 8. Pairing results HADER-lidar.

Figure 9 shows the computation results of the reference speed and its associated uncertainty from the multiple sensors output using the data fusion and polynomial interpolation modules. We observe a good matching between HADER measurements and the reference speed values. The absolute differences do not exceed the uncertainty level of the system assigned at 0.34 km/h, except for 10 % of the measurements. It is assumed that is due to a false pairing of targets between HADER and the multi-sensor cinemometer system.

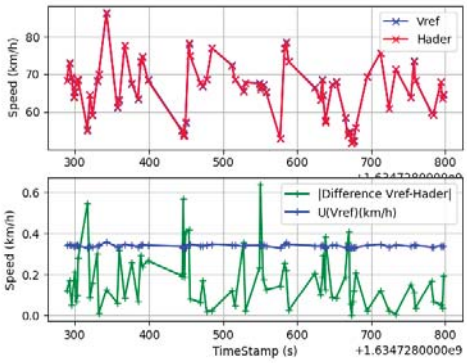

Fig. 9. Computation results of the reference speed and its associated uncertainty.

VI. CONCLUSION

In this article, the design of reference multi-sensor cinemometer is described. The system performance has been verified by comparison to the actual reference cinemometer. The system uses a multi-sensor approach already implemented for traffic control applications [6]. The data acquisition and processing units of this system provide an extended set of features with the combination of radar and lidar technologies capabilities. The processing unit includes sensor's data fusion, regression model and predictions of the speed values before, after and at the infraction line. The localization of this measurement point is software-defined within the measurement range of the sensors, which allows a greater flexibility for the exploitation of the measurement results. The data processing module allows to compute the measurement uncertainty associated to the reference speed value. On-site measurements have been performed to compare the system with the reference system HADER. The results show a good agreement with the existing reference cinemometer.

REFERENCES

[1] M.I.Skolnik, "Introduction to radar", Radar handbook, 1962, vol. 2, p. 21.

[2] K.K.M Shariff, E.Hoare, L.Daniel, et al., "Comparison of adaptive spectral estimation for vehicle speed

Table 2. Mean (μ) and standard deviation (σ) of relative difference of paired speed values of HADER and the multi-sensor cinemometer system with varying test conditions.

		Test 1 10min	Test 2 10 min	Test 3 10 min	Test 4 20 min	Test 5 30 min
HADER-Radar 1	$\mu(\%)$	0.15	0.19	0.21	0.13	0.18
	$\sigma(\%)$	0.4	0.4	0.47	0.39	0.47
HADER-Radar 2	$\mu(\%)$	-0.05	-0.1	0	-0.09	0.03
	$\sigma(\%)$	0.33	0.46	0.38	0.42	0.49
HADER-Radar 3	$\mu(\%)$	-0.21	-0.2	-0.11	-0.23	-0.27
	$\sigma(\%)$	0.39	0.48	0.44	0.43	0.49
HADER-Radar 4	$\mu(\%)$	-0.01	-0.12	0.1	-0.02	-0.08
	$\sigma(\%)$	0.43	0.44	0.44	0.43	0.52
HADER-Lidar	$\mu(\%)$	0.18	0.06	0.08	0.13	0.16
	$\sigma(\%)$	0.51	0.52	0.47	0.54	0.57

measurement with radar sensors", Sensors, 2017, vol. 17, no 4, p. 751.

[3] Q.Agrabat, A.Batailly, "Cubic and bicubic spline interpolation in Python", Doctoral dissertation, École Polytechnique de Montréal, 2020.

[4] P.Hindle, "Comprehensive Survey of 77, 79 GHz Automotive Radar Companies-Sensors and ICs", Microwave Journal, March 2020.

[5] M.J.T.Milton, P.M.Harris, I.M.Smith, et al., "Implementation of a generalized least-squares method for determining calibration curves from data with general uncertainty structures", Metrologia, 2006, vol. 43, no 4, p. S291.

[6] M.Wang, L.Jiang, W.Lu, et al., "Detection and tracking of vehicles based on video and 2D radar information", International Conference on Intelligent Transportation. Springer, Singapore, 2016. p. 205-214.